Journal Pre-proofs

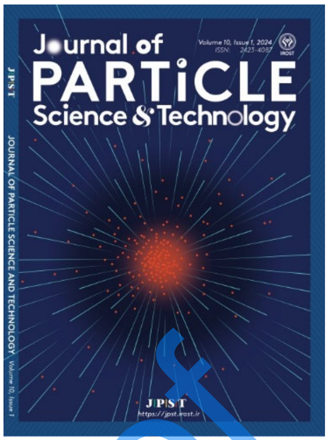

Ultrasonic assisted cold compaction of CP-Titanium and Ti-6Al-4V alloy

Vahid Fartashvand, Rezvan Abedini, Raheleh KhanMohammadi, Amir Abdullah, Nader Parvin

DOI: https://doi.org/10.22104/jpst.2024.7089.1262
Manuscript number: JPST-2409-1262

To appear in: *Journal of Particle Science and Technology (JPST)*

Received Date: 8 September 2024

Received Date in revised form: 10 November 2024

Accepted Date: 18 November 2024

Please cite this article as: Fartashvand V., Abedini R., Khanmohammadi R., Abdullah A., Parvin N., Ultrasonic assisted cold compaction of CP-Titanium and Ti-6Al-4V alloy, *Journal of Particle Science and Technology* (2024), doi: https://doi.org/10.22104/jpst.2024.7089.1262

Ultrasonic assisted cold compaction of CP-Titanium and Ti-6Al-4V alloy

Vahid Fartashvand[a,*], Rezvan Abedini[b], Raheleh KhanMohammadi[c], Amir Abdullah[c], Nader Parvin[d]

[a] Department of Industrial Design, Faculty of Art, Alzahra University, Tehran, Iran

[b] Department of Mechanical Engineering, University of Science and Technology, Tehran, Iran

[c] Department of Mechanical Engineering, Amirkabir University of Technology, Tehran, Iran

[d] Materials and Metallurgical Engineering Department, Amirkabir University of Technology, Tehran, Iran

Abstract

Superimposed ultrasonic vibration during compaction of CP-Titanium and Ti-6Al-4V alloy improves the relative density and quality of the compact. The underlying mechanisms of this process are not well understood. In this study, the influence of ultrasonic vibrations on the densification behavior of square packing of Ti-6Al-4V and CP-Ti powders during cold compaction was investigated using the Multi-Particle Finite Element Method (MPFEM). The acoustic softening and friction reduction were introduced in this model. The density-pressure curves show that ultrasonic vibration improves the densification of these powders, owning to the acoustic softening that leads to a decline in the required pressure. It has been found that the ultrasonic effect on reducing the compaction pressure and stress in the case of pure titanium is greater than that of titanium alloy. In addition, an increase in the intensity and amplitude of ultrasonic vibration reduces stress. The rotation and rearrangement of the particles caused by the reduction of friction lead to an enhancement in the compression capability.

Keywords: Multi-Particle Finite Element, Cold consolidation, High power ultrasonic vibration, Acoustic softening

1. Introduction

Titanium and its alloys have appropriate properties such as high specific strength, high corrosion resistance, and biocompatibility. Therefore, they are widely used in the chemical, medical, aero, and jewelry industries [1,2]. Due to the high cost of these materials, powder metallurgy (PM) as a near-net-shape manufacturing technology that has been widely used to fabricate components [3,4]. In addition, easy operation and a high production rate are other advantages of PM technology. Press and sintering is the most straightforward technology among powder metallurgy techniques [5]. In this operation, the powder is pressed into a desirable shape, and then the compacted part is sintered. Inter-particle friction and die wall friction decreases the effective pressure along with the component thickness, and this pressure gradient induces inhomogeneous density distribution in compacted bodies. Shape distortion after sintering is the main result of this density variation. To overcome this problem, ultrasonic vibration successfully was superimposed on the compaction of titanium powders [6,7,8]. Ultrasonic vibration causes the reduction of friction force at contacting surfaces [9] and diminishes the pressure gradient along the compacted part. In addition, the reduction of flow stress during superimposing ultrasonic vibration (as called acoustic softening) decreases forming forces [10]. As another benefit, heat generation at the contacting surface due to absorption of ultrasonic vibration increases the compressibility of powders [11,12,13]. These advantages incentive using ultrasonic vibration during powder consolidation of low compressibility powders. Therefore, any improvement of the compaction processes of powders leads to high-quality compacted parts and thus increases the mechanical properties of the final piece.

Densification of the powder mass depends on various parameters such as the elastic-plastic properties of particles, the size and morphology of particles, the particle configuration, the inter-particle friction, the friction between the particles and the die walls, and loading. The role of each parameter on the powder densification behavior is not easily obtainable in the experimental tests due to their interaction. Also, compaction pressure, lubricant, sintering temperature, and sintering time [14,15] are the main parameters of powder compaction process. The relative density of the titanium green compact is directly proportional to the compaction pressure. These frictional effects can be reduced by use of suitable lubricant [16]. Sintering is one of the most critical steps of powder metallurgy. Time and temperature of Sintering, sintering atmosphere as well as heating rate could influence of mechanical properties of compacted part.

Numerical modeling with the ability to modify a parameter according to the intended behavior is valuable for understanding densification mechanisms.

Two basic procedures have been used for the numerical modeling of the powder compaction process, namely the discrete element method (DEM) and the finite element method (FEM). In DEM, each particle is modeled, and Newton's laws calculate the adjacent particle's interaction. By the progression of the compaction process, contact and separation between the particles are detected. In FEM, the porous constitute equation of material is considered, but the rotational spin and particle rearrangement are neglected [17]. In recent years, the multi-particle finite element method (MPFEM) has been proposed and used to simulate powder compaction. The advantage of MPFEM lies in that it combines the features of traditional FEM and DEM and can successfully simulate the compaction densification of powders with large deformation from a particulate scale [18,19]. The MPFEM method is modeled as deformable continuum material, and their interactions are considered. The interaction between the neighboring particles is calculated based on DEM, and their deformation is calculated with FEM.

Many research works have been reported on powder compaction using an MPFEM. Procopio *et al.* [17] applied the MPFEM approach to investigate the multi-axial condensation of granular mass from weak to high relative densities in 2D. Their work demonstrates that the MPFEM model is beneficial in explaining inter-particle behavior and its impact on the microscopic and macroscopic response in different strain histories. Kim *et al.* [20] used the MPFEM method to observe the deformation behavior of Aluminum particles and estimate the relative density for different punch speeds and particle diameters. Huang *et al.* [18] used MPFEM to numerically study the 2D compaction of binary Al/SiC composite powders. Different initial packing structures with various Al/SiC particle size ratios and compositions are constructed and imported into a FEM model for compaction. Their results show that initial powder packing configurations determine the densification process and the properties of the compacts. Mei *et al.* [21] simulated the densification of Al and NaCl powders by CZM-based MPFEM. They simulated the fracture of particles by this method. Han *et al.* [22] simulated 2D compaction of Fe-Al composite powders by MPFEM at different size ratios. Korim and Hu [19] studied spongy copper powder densification and compaction mechanisms using a multi-particle finite element method. Zhou *et al.* [23] used MPFEM to determine green density and impact energy relation in Ti-6Al-4V powders. Ji *et al.* [24] simulated the hot-pressing densification of (SiCp)/6061Al composite powders. In this study, the influence of ultrasonic vibration on the compaction of Ti-6Al-4V and CP-Ti was investigated by computer simulation. This study is a part of our investigation on ultrasonic-assisted powder cold/hot compaction. Up to date, no study about the MPFEM of ultrasonic-assisted compaction has been published. We focus our paper on mono-size circular particles to investigate the influence of ultrasonic vibration (acoustic softening and friction reduction) on compaction efficiency. Better understating of ultrasonic-assisted cold compaction leads to improved green part quality and therefore increases final product quality.

2. Simulation Procedure and Condition

In this simulation, the densification behavior of particles under uniaxial pressing without ultrasonic vibration and associated with superimposed ultrasonic vibration was analyzed by MPFEM. The simulation was conducted using finite element software ABAQUS/Explicit. An explicit integration scheme was used because it is appropriate for the contact problems and high degree of freedom systems. Also, the system is modeled as a two-dimensional plane strain. As an essential step in finite element numerical modeling, desirable mesh (size and type) must be selected. Different mesh types and sizes were used (as shown in Figure 1). In a mesh sensitivity study, a deformable particle is modeled between upper and lower punches to decrease simulation cost. Then by applying compression force at a rigid upper punch, the force-displacement curve (Figure 2) and Von-Mises effective stress (Figure 3) were extracted. Transient mesh (as shown in Figure 1-H) was chosen by considering simulation cost and accuracy.

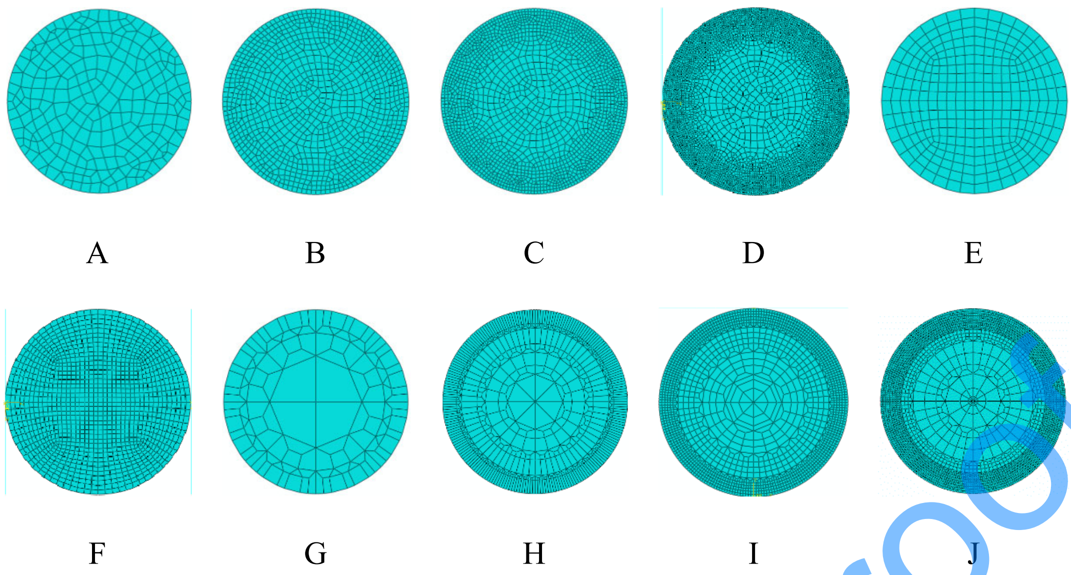

Figure 1. Mesh sensitivity analysis: A) coarse free mesh, B) medium free mesh [25], C) fine free mesh, D) very fine free mesh, E) coarse structural mesh [26], F) fine structural mesh, G) coarse transient mesh [9], H) transient mesh, I) fine transient mesh and J) very fine transient mesh [27].

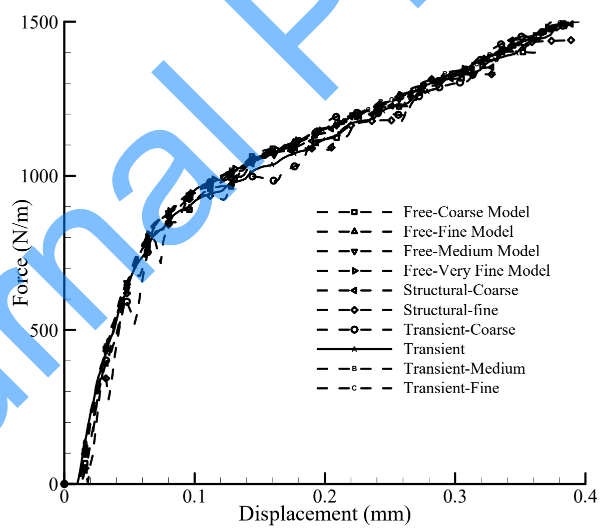

Figure 2. The effect of mesh size and type on force-displacement curves of upper punch.

In the next step, the accuracy of the simulation was investigated by using Wu *et al.* [14] experimental work. Other authors [28] used their results to verify the simulation shown in Figure 4.

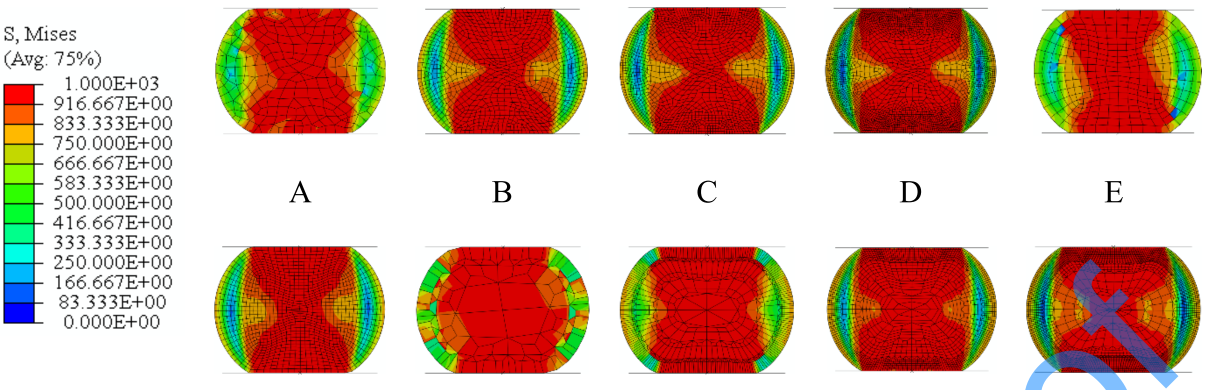

Figure 3. Stress distribution during mesh sensitivity analysis: A) coarse free mesh, B) medium free mesh [12], C) fine free mesh, D) very fine free mesh, E) coarse structural mesh [13], F) fine structural mesh, G) coarse transient mesh [9], H) transient mesh, I) fine transient mesh and J) very fine transient mesh [14].

As shown from these curves, there is a good agreement between simulation and experimental data. So, the modeling procedure has significant accuracy in simulating a collection of particles. Large mesh size causes fluctuation in this curve, so a smooth curve indicates a suitable mesh size.

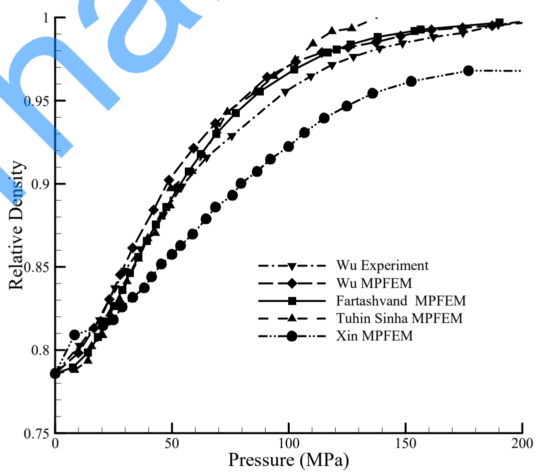

Figure 4. Relative density versus compression pressure in order to verification of simulation method.

The finite-discrete element modeling has many computations due to the existence of many distinct particles with geometry and nonlinear behavior, namely elastic-plastic deformation and the presence of many contact surfaces. In this study, a cylindrical die with 12mm diameter and 12mm height was modeled. The number of particles that can be modeled is determined by the CPU and RAM restrictions in addition to the number of particle-particle contact pairs. Therefore, sixty-four circular particles with a diameter of 1.5mm were considered for compaction. These numbers are enough to investigate inter-particle friction, die-wall friction and, rearrangement of powders. The die walls and lower punch were rigid, and their displacement was restricted in all directions. Displacement boundary condition was imposed on rigid upper punch. In order to calculate instantaneous relative density, the displacement of the upper punch was used. Experimental compression data measured mechanical properties of Ti-6Al-4V, and the effect of superimposed ultrasonic vibration on this material was extracted from the authors' previous works, [29, 30] and material property of CP-Ti was extracted by using stress superposition theory from Ref. [31]. The inter-particle contacts and the particle and die wall contacts were considered via a kinematic contact algorithm. The Coulomb friction theory was used. The inter-particle friction coefficient and the die wall friction coefficient with particles for both simulations of Ti-6Al-4V and CP-Ti powders were set at 0.28 and 0.4, respectively [32]. Regarding the large deformation of elements during compaction processes, the adaptive mesh technique was used with 60 frequencies. The effect of punch speed (simulation time) was investigated, and consequently, 0.05s time was selected for the simulation time.

To investigate the acoustic softening influence of ultrasonic vibrations in simulations, the Ti-6Al-4V alloy tensile test was performed under ultrasonic vibrations at two intensities of 100W and 340W [17]. For CP titanium, the stress-strain curve under ultrasonic vibration was extracted from [18] for three vibrational amplitudes of 0µm, 5.6µm, and 6.4µm. The relationship between the power (P) and amplitude of vibration (A) is as follow:

$$P = \frac{1}{2} A^2 \omega^2 \rho c \quad (1)$$

Which ω is the angular frequency, ρ is density and c sound velocity in material.

To apply the ultrasonic effect on the friction in simulations, the friction coefficient is assumed to be zero in the presence of ultrasonic vibrations.

3. Results and discussion

3.1. Comparison of Ultrasonic Effects on CP Titanium and Ti-6Al-4V Alloy

Compression pressure (P) plays a dominant role among many factors that can affect compaction. Here, P is referred to as the average pressure imparted to the upper punch. Figure 5 shows the relationship between compaction pressure and upper punch displacement for three vibrational modes ((a) Ti-6Al-4V alloy and (b) CP titanium). It can be seen in both curves that by moving the upper punch down, at first, the amount of pressure increases gradually, and after about 2.5mm displacement, the rate of increase in compaction force is increased. It is observed that the effect of ultrasonic vibrations on reducing the force required for powder compaction of CP titanium is greater than that of Ti-6Al-4V alloy.

Figure 6 shows the relationship between pressure and relative density for the Ti-6Al-4V and CP titanium. The relative density begins with the initial value of 0.78 and reaches the full density under compaction pressure.

Investigation of the behavior of Ti-6Al-4V alloy in three ultrasonic intensities (Figure 6-a) showed that a relative density of 0.8 at ultrasonic powers of 0W, 100W, and 300W is obtained at compaction pressures of 411MPa, 401MPa, and 388MPa, respectively. Consequently, at a relative density of 0.8, the required pressure is reduced by about 10MPa (2.4%) and 13MPa (5.5%) by ultrasonic intensities of 100W and 300W, respectively. In the case of CP titanium (Figure 6-b), the relative density of 0.8 in the vibrational amplitudes of 0µm, 5.6µm, and 6.4µm is obtained at compression pressures of 208MPa, 153MPa, and 105MPa, respectively. Thus, at this relative density, the vibrational amplitudes of 5.6µm and 6.4µm reduced the required pressure 55MPa (26%) and 103MPa (49.5%). Also, the ultrasonic effects on reducing required pressure in pure titanium are more significant than in titanium alloy. The effect of acoustic softening has been leading to reduce the required pressure, as the relative density of 0.92 for CP titanium was obtained at vibration amplitudes of 5.6μm and 6.4μm with lower pressures of 183MPa and 311MPa, respectively, which indicates the effectiveness of ultrasonic vibrations in improving the densification behavior of the material. This pressure reduction compared to conventional compression (without ultrasonic) is observed up to 99.7% relative density.

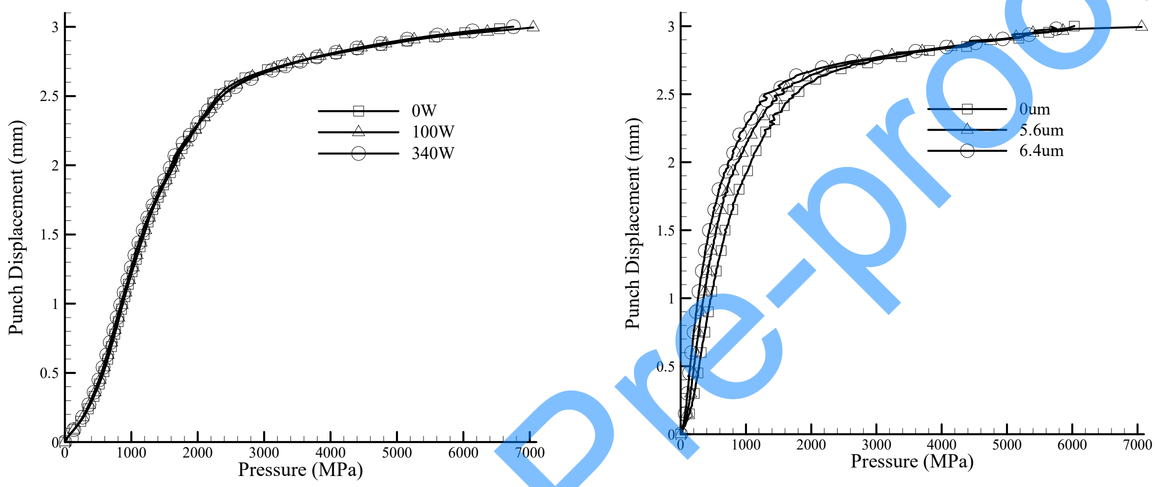

(a) (b)

Figure 5. Punch displacement versus compaction pressure for: a) Ti-6Al-4V alloy and b) CP titanium.

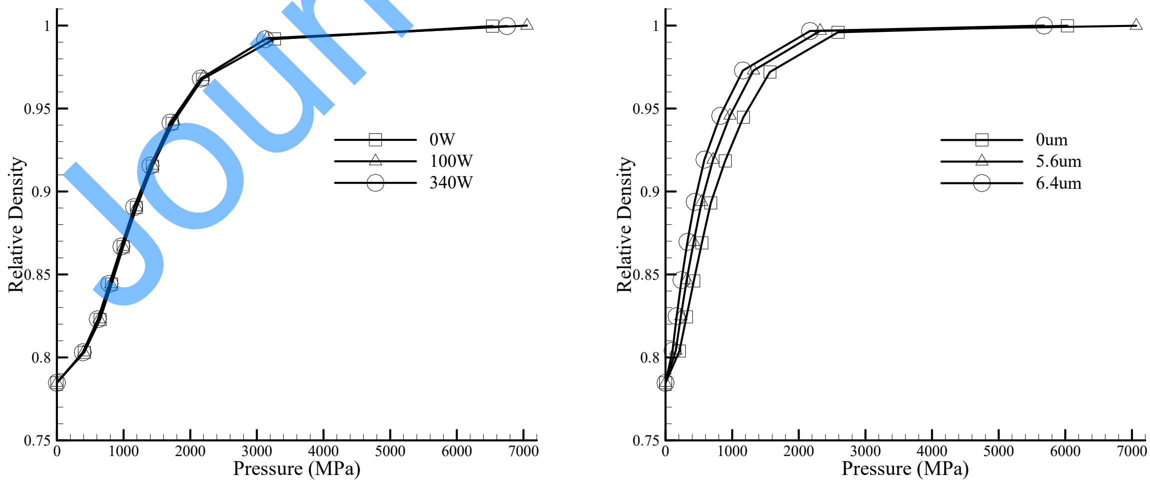

(a) (b)

Figure 6. Relative density versus compaction pressure for: a) Ti-6Al-4V alloy and b) CP titanium.

3.2. Macrostructure characterization during compaction

Figure 7 and Figure 8 indicate the evolution of morphology, local packing structure, and equivalent Von Mises stress for CP titanium and Ti-6Al-4V particles during compaction. The compression of Ti-6Al-4V needs more pressure than CP-Ti due to its higher strength. The pressure increases rapidly at the early stage of compaction. No apparent relative slip between particles for cases is observed due to the highly geometrical symmetry of the initial packing. It is also seen that at the early stages of compaction, the localized deformation of the particles leads to the formation of a stress chain. Due to that, the particles are modeled as elastic-plastic. The plastic deformation begins with reaching equivalent Von Mises stress to yield stress. Accordingly, it is observed that all the particles have a plastic deformation, and they do not retain their original shape. So that, with the further increase in the pressure, large plastic deformation of particles occurred and the in-plane forces between neighboring particles formed and increased. In this duration, the contact between particles changes from point to arc. The significant plastic deformation results in the mass transfer of particles to fill adjacent low pressured void area for densification.

Relative density and uniform density distribution of a compacted powders determines the green strength, sintering rate, final density, shrinkage and the distortion during sintering. Higher relative density of powder compact results in higher green strength and higher relative density of sintered part. Uniform density distribution causes to lower shrinkage and distortion during sintering. So, reducing inter-particle's voids causes to good properties of sintered parts. The particles in contact with the die walls deform non-uniformly due to the friction force, and they undergo more deformation on the one side and less stress on the other side. After compaction, the shapes of particles in the compacts are near rectangular. From the comparison of Von Mises stress in morphological evolution on the compaction of pure titanium and Ti-6Al-4V alloy powders, it can be seen that ultrasonic vibrations lead to decreases in stress. Also, by increasing the amplitude and intensity of ultrasonic, its effect reduces stress. These observations indicate the impact of ultrasonic acoustic softening.

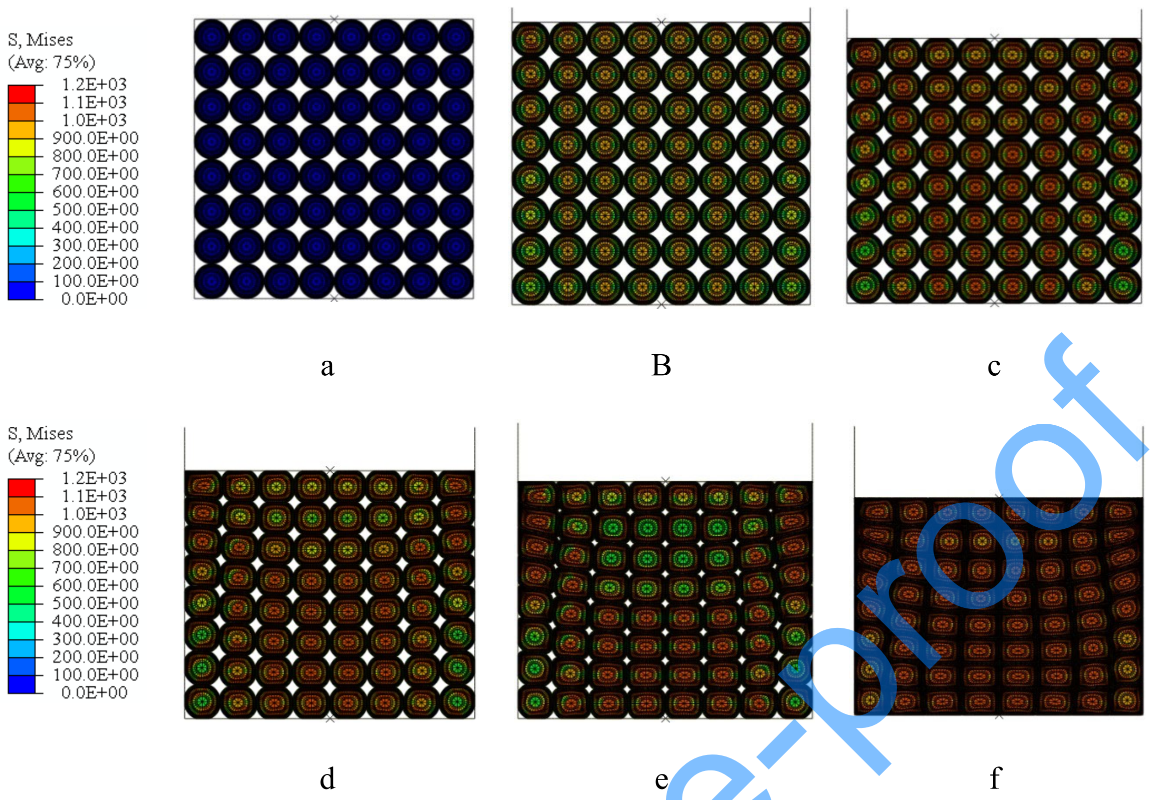

Figure 7. Evolution of morphology, local packing structure and equivalent von mises stress without ultrasonic vibration for Ti-6Al-4V during compaction in the punch displacement at the amount of: a) 0mm, b)0.6mm, c) 1.2mm, d) 1.8mm, e) 2.4mm and f) 3mm.

The major benefit of the MPFEM model is its ability to obtain information regarding the local stress and strain state at the inter-particle contact area. To study the ultrasonic effect of friction reduction, friction was considered zero, and simulations were performed for both Ti-6Al-4V and CP titanium. Figure 9 and Figure 10 show that the distribution of equivalent Von Mises stress is shown in the frictionless model for Ti-6Al-4V and CP titanium, respectively. Due to the friction removal, the possibility of the rotation and displacement of the particles is provided, and the position of the particles in the radial direction of the die has been changed. In contrast, there is no such rotation and displacement for compaction with the presence of friction. This phenomenon indicates how much friction affects the particle rearrangement stage. In other words, rotating and rearrangement of the particles caused by removing friction led to increased compression capability.

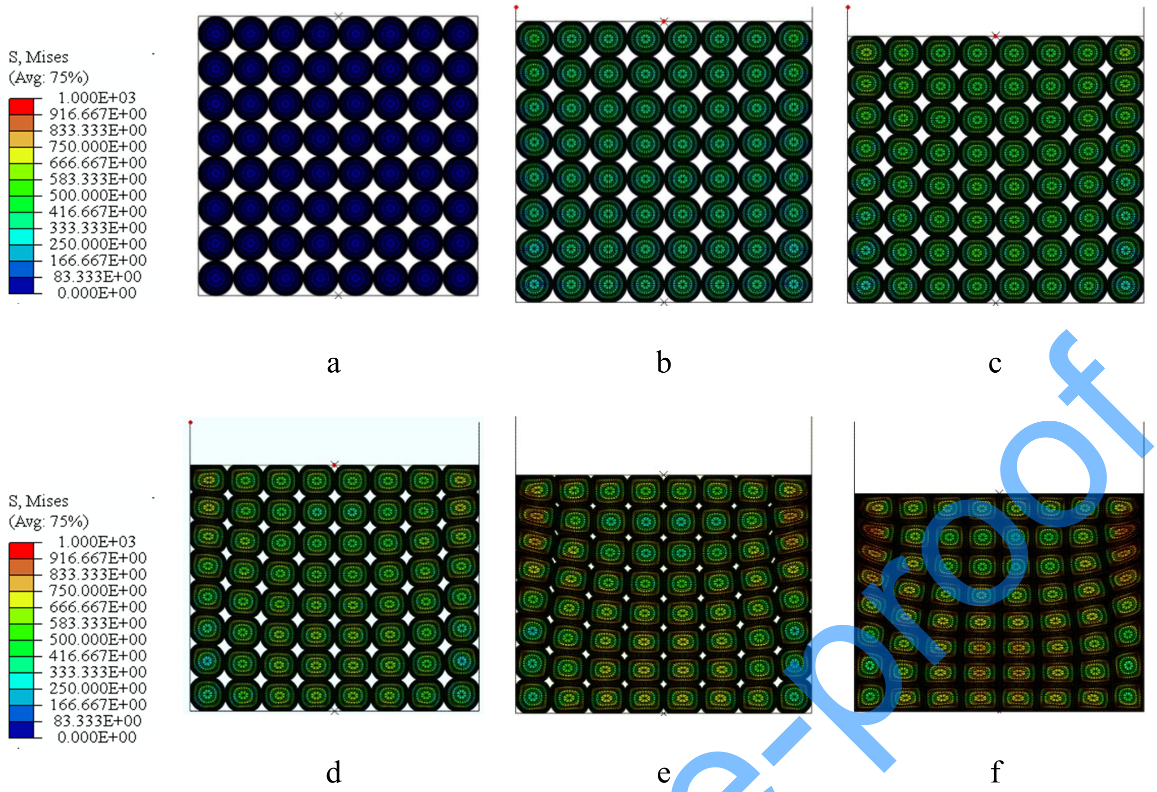

Figure 8. Evolution of morphology, local packing structure and equivalent von mises stress without ultrasonic vibration for CP-Titanium during compaction in the punch displacement at the amount of: a) 0mm, b) 0.6mm, c) 1.2mm, d) 1.8mm, e) 2.4mm and f) 3mm.

Investigation of the behavior of Ti-6Al-4V alloy showed that for achieving the relative density of 0.8, 0.89, and 0.99, the amount of pressure was reduced 31MPa, 525MPa, and 814MPa by removing friction. In the case of CP titanium, it is observed that the pressure was reduced 25MPa, 260MPa, and 517MPa by removing friction for achieving the relative density of 0.8, 0.89, and 0.99, respectively. Using ultrasonic Vibration can produce high density green parts and fairly uniform density distribution of them with long tool's lifetime. In Ti-6Al-4V, the effect of friction between particles and friction between particles and die walls was also investigated (each time one of them was considered zero). The results indicate that removing friction between the particles is more effective than eliminating friction between particles and die wall in reducing the required pressure of compaction. So, ultrasonic vibrations have a beneficial influence in improving the densification behavior of the material.

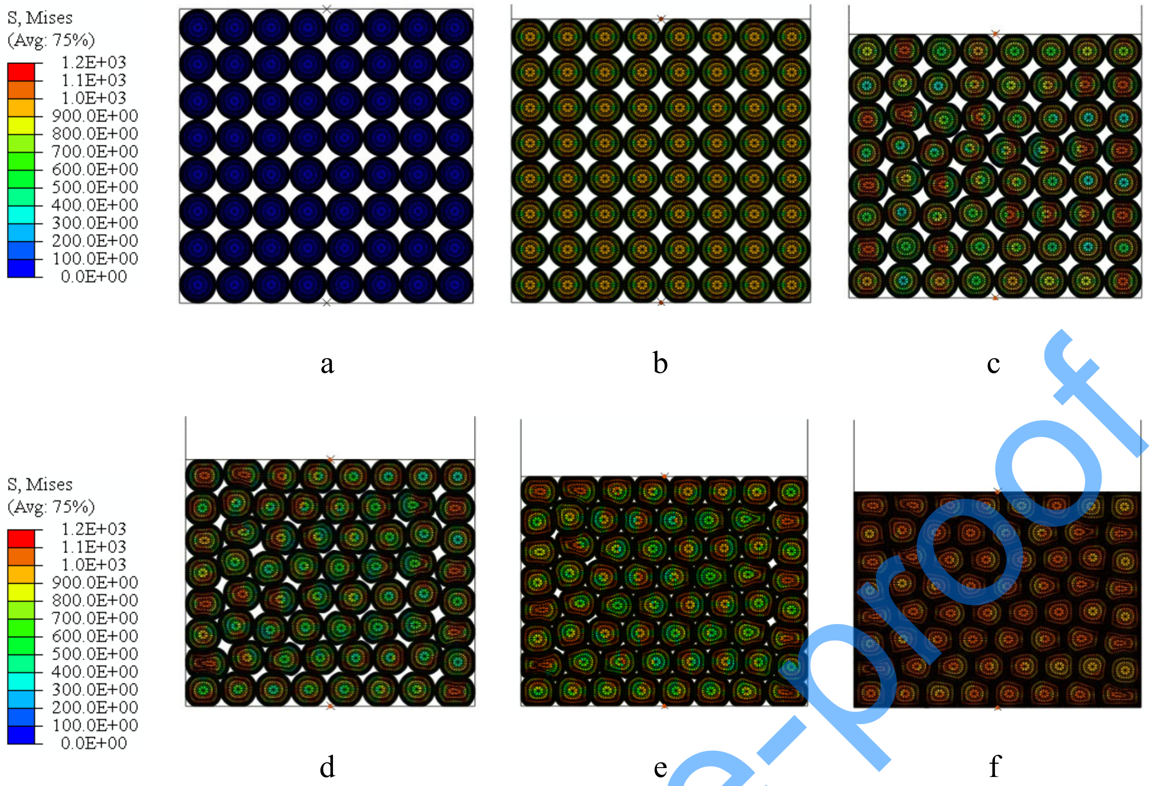

Figure 9. Evolution of morphology, local packing structure and equivalent Von Mises stress for Ti-6Al-4V alloy during frictionless compaction in the punch displacement at the amount of: a) 0mm, b) 0.6mm, c) 1.2mm, d) 1.8mm, e) 2.4mm and f) 3mm.

4. Conclusions

The use of the multi-particle finite element model (MPFEM) offers an exciting insight into the compaction of particles. As a result, this model can address rearrangement, particle rotation, and large deformation to high relative densities.

In this research, in the following of our previous published papers, the compression behavior of Ti-6Al-4V and CP titanium was investigated under a uniaxial longitudinal superimposed ultrasonic vibration condition. Ultrasonic vibration was modeled as acoustic softening in material properties and friction reduction. Form results, the following were concluded:

(a) It is observed that ultrasonic vibration decreases the required pressure for compaction. This enhancement in CP titanium was greater than Ti-6Al-4V alloy.

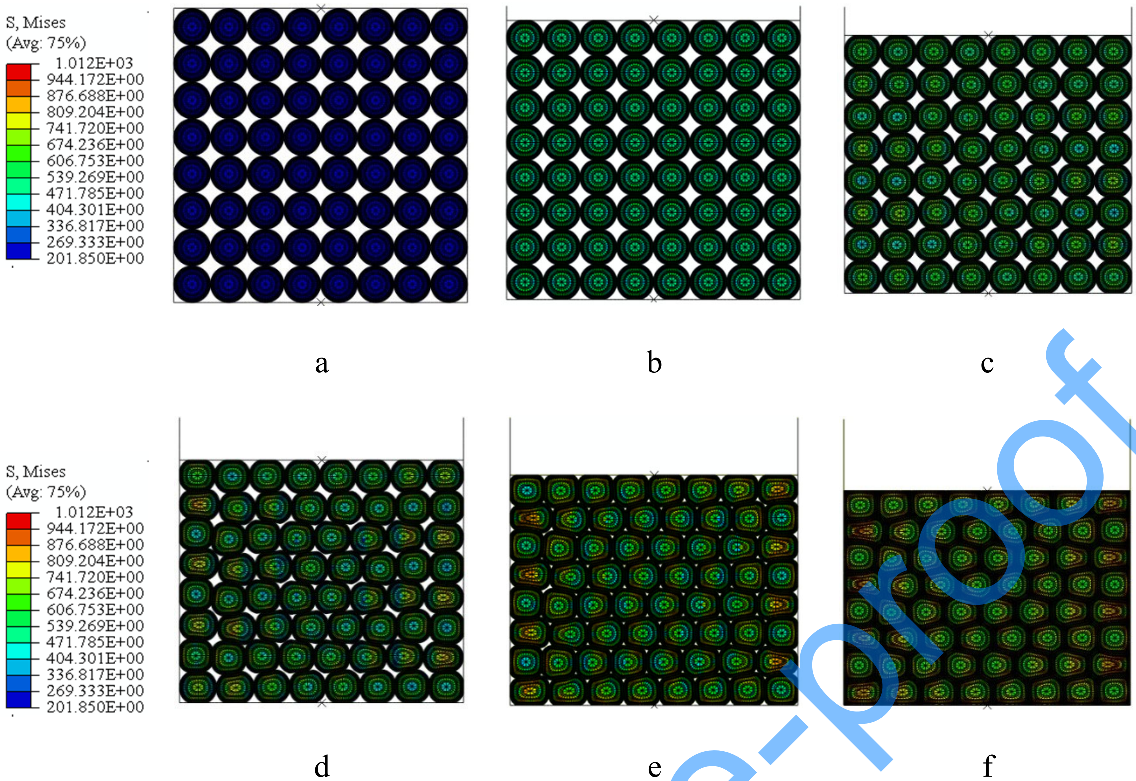

Figure 10. Evolution of morphology, local packing structure and equivalent Von Mises stress for CP titanium during frictionless compaction in the punch displacement at the amount of: a) 0mm, b) 0.6mm, c) 1.2mm, d) 1.8mm, e) 2.4mm and f) 3mm.

(b) It is observed that ultrasonic vibration decreases the required pressure for compaction. This enhancement in CP titanium was greater than Ti-6Al-4V alloy.

(c) Higher intensity and amplitude of the ultrasonic will increase its effectiveness in reducing compaction pressure.

(d) Rotating and rearrangement of the particles caused by the reduction of friction lead to increased compression capability.

(e) The results indicate that removing friction between the particles is more effective than eliminating friction between particles and die wall in reducing the required compaction pressure.

Acknowledgemnt

The authors express their sincere appreciation to Dr. Yunes Alizadeh and Dr. Nader Parvin for their help and support. Thanks also be given to Farasou Tajhiz Iranian Co. No funding

Conflict of Interest

The authors declare that they have no known competing financial interests or personal relationships that could have appeared to influence the work reported in this paper.

References

[1] M. J. Donachie, Titanium: a technical Guide, second ed., ASM International, 2000.

[2] S. Amini, M. Farzin, A. Mohammadi, An Experimental Study on Ultrasonic-assisted Hot Incremental Sheet Metal Forming of Ti–6Al–4V, Iran. J. Sci. Technol. - Trans. Mech. Eng. (2023) https://doi.org/10.1007/s40997-023-00602-8.

[3] P.G. Esteban, Y. Thomas, E. Baril, E. M. Ruiz-Navas, E. Gordo, Study of Compaction and Ejection of Hydrided-Dehydrided Titanium Powder, Met. Mater. Int. 17 (2011) 44–45. https://doi.org/10.1007/s12540-011-0207-z

[4] Y. Liu, L. F. Chen, H. P. Tang, C. T. Liu, B. Liu, B. Y. Huang, Design of powder metallurgy titanium alloys and composites, Mat. Sci. Eng. A-Struct. 418 (2006) 25–35. https://doi.org/10.1016/j.msea.2005.10.057

[5] M. Qian, F. H. Froes, Titanium Powder Metallurgy Science, Technology and Applications, First ed., Elsevier Science, 2015.

[6] V. Fartashvand, A. Abdullah, S. A. Sadough Vanini, Effects of high power ultrasonic vibration on the cold compaction of titanium, Ultrason. Sonochem. 36 (2017) 155-161. https://doi.org/10.1016/j.ultsonch.2016.11.017

[7] V. Fartashvand, R. Abedini, A. Abdullah, Influence of ultrasonic vibrations on the properties of press-and-sintered titanium, Proc. Inst. Mech. Eng. B J. Eng. Manuf. 2022,

https://doi.org/10.1177/09544054221078386.

[8] R. Abedini, V. Fartashvand, A. Abdullah, Y. Alizadeh, Evaluation of process parameters and ultrasonic vibration in hot pressing of metal powders, Materials Science and Engineering: B. 281 (2022) 115731. https://doi.org/10.1016/j.mseb.2022.115731.

[9] S. Dong, M. J. Dapino, Elastic–plastic cube model for ultrasonic friction reduction via Poisson's effect, ULTRASONICS. 54 (2014) 343–350. https://doi.org/10.1016/j.ultras.2013.05.011

[10] B. Meng, B. N. Cao, M. Wan, C. J. Wang, D. B. Shan, Constitutive behavior and microstructural evolution in ultrasonic vibration assisted deformation of ultrathin superalloy sheet. Int. J. Mech. Sci. 157-158 (2019) 609-618. https://doi.org/10.1016/j.ijmecsci.2019.05.009

[11] P. Sancin, O. Caputo, C. Cavallari, N. Passerini, L. Rodriguez, M. Cini, A. Fini, Effects of ultrasound-assisted compaction on Ketoprofen/ Eudragit S100 Mixtures, Eur. J. Pharm. Sci. 7 (1999) 207-213. https://doi.org/10.1016/S0928-0987(98)00022-0

[12] R. Abedini, A. Abdullah, Y. Alizadeh, V. Fartashvand, A Roadmap for Application of High Power Ultrasonic Vibrations in Metal Forming, Modares Mechanical Engineering 16 (2017) 323-334.

[13] R. Abedini, V. Fartashvand, A. Abdullah, Y. Alizadeh, Finite element modelling of ultrasonic assisted hot pressing of metal powder. Mechanics of Time-Dependent Materials (2024) https://doi.org/10.1007/s11043-024-09735-y

[14] N. Kumar, A. Bharti, K. K. Saxena, A re-investigation: Effect of powder metallurgy parameters on the physical and mechanical properties of aluminium matrix composites, Mater. Today, 44 (2021) 2188-2193. https://doi.org/10.1016/j.matpr.2020.12.351

[15] I. Kaseb, M. Moazami-Goudarzi, A. R. Abbasi, Effect of Particle Size on the Compressibility and Sintering of Titanium Powders, Iranian Journal of Materials Forming 6 (2019) 42-51 https://doi.org/10.22099/ijmf.2019.34264.1134

[16] S.M.Zahraee. Experimental Investigation of Metal Powder Compaction without Using Lubricant, Journal of Particle Science and Technology 2 (2016) 141-149 http://dx.doi.org/10.22104/jpst.2016.445

[17] A. T. Procopio, A. Zavaliangos, Simulation of multi-axial compaction of granular media from loose to high relative densities, J. Mech. Phys. Solids, 53 (2005) 1523-1551. https://doi.org/10.1016/j.jmps.2005.02.007

[18] F. Huang, X. An, Y. Zhang, A. Yu, Multi-particle FEM simulation of 2D compaction on binary Al/SiC composite powders. Powder Technology 314 (2017) 39-48. https://doi.org/10.1016/j.powtec.2017.03.017

[19] N. S. Korim, L. Hu, Study the densification behavior and cold compaction mechanisms of solid particles-based powder and spongy particles-based powder using a multi-particle finite element method, Mater. Res. Express, 7 (2020) 056509. https://doi.org/10.1088/2053-1591/ab8cf6

[20] K. H. Lee, J. M. Lee, B. M. KIM, Densification simulation of compacted Al powders using multi-particle finite element method, T NONFERR METAL SOC. 19 (2009) s68-s75. https://doi.org/10.1016/S1003-6326 (10) 60247-6

[21] Y. Feng, D. Mei, Y. Wang, Cohesive zone method based multi particle finite element simulation of compaction densification process of Al and NaCl laminar composite powders. J Phys Chem Solids. 134 (2019) 35-42. https://doi.org/10.1016/j.jpcs.2019.05.020

[22] P. Han, X. An, D. Wang, H. Fu, X. Yang, H. Zhang, Z. Zou, MPFEM simulation of compaction densification behavior of Fe-Al composite powders with different size ratios. J. Alloys Compd. 741 (2020) 473–481. https://doi.org/10.1016/j.jallcom.2018.01.198

[23] J. Zhou, Ch. Zhu, W. Zhang, W. Ai, X. Zhang, K. Liu, Experimental and 3D MPFEM simulation study on the green density of Ti–6Al–4V powder compact during uniaxial high velocity compaction. J. Alloys Compd. 817 (2020) 153226. https://doi.org/10.1016/j.jallcom.2019.153226

[24] L. Xu, Y. Wang, Ch. Li, G. Ji, G. Mi, MPFEM simulation on hot-pressing densification process of SiC particle/6061Al composite powders. J Phys Chem Solids. 159 (2021) 110259. https://doi.org/10.1016/j.jpcs.2021.110259

[25] G. Gustafsson, H.A. Häggblad, P. Jonsén, Multi-particle finite element modelling of the compression of iron ore pellets with statistically distributed geometric and material data, Powder

Technology 239 (2013) 231-238. https://doi.org/10.1016/j.powtec.2013.02.005

[26] Y.X. Zhang, X.Z. An, Y.L. Zhang, Multi-particle FEM modeling on microscopic behavior of 2D particle compaction, Applied Physics A, 118 (2015) 1015–1021. https://doi.org/10.1007/s00339-014-8861-x

[27] W. Wu, G. Jiang, R. H. Wagoner, G. S. Daehn, Experimental and numerical investigation of idealized consolidation part 1: static compaction, Acta Materialia 48 (2000) 4323–4330. https://doi.org/10.1016/S1359-6454(00)00206-8

[28] X. J. Xin, P. Jayaraman, G. S. Daehn, R. H. Wagoner, Investigation of yield surface of monolithic and composite powders by explicit finite element simulation, Int. J. Mech. Sci. 45 (2003) 707–723. https://doi.org/10.1016/S0020-7403(03)00107-3

[29] V. Fartashvand, A. Abdullah, S. A. Sadough Vanini, Investigation of Ti-6Al-4V alloy acoustic softening. ULTRASON. SONOCHEM. 38 (2017) 744-749. https://doi.org/10.1016/j.ultsonch.2016.07.007

[30] M. Sadeghi; V. Fartashvand; A. Abdullah; A.R. Fallahi Arezoodar; R. Abedini, Experimental investigation of vibrational mode shape influence on compression behaviour of Ti-6Al-4V alloy under superimposed ultrasonic vibration. Journal of solid and fluid mechanics. 12 (2022) 55-68. https://doi.org/10.22044/jsfm.2022.11100.3452

[31] H. Zhou, H. Cui, Q. Qin, H. Wang, Y. Shen, A comparative study of mechanical and microstructural characteristics of aluminium and titanium undergoing ultrasonic assisted compression testing, Mater. Sci. Eng. A, 682 (2017) 376–388. https://doi.org/10.1016/j.msea.2016.11.021

[32] R. Boyer, G. Weisch, E. W. Collings, Material Properties Handbook Titanium Alloys, ASM International, 1994.